Supplementary Materials

Stroboscopic neutron diffraction applied to fast time-resolved operando studies on Li-ion battery (d-$LiNi_{0.5}Mn_{1.5}O_4$ vs. graphite)

Denis Sheptyakov[1*], Lucien Boulet-Roblin[2], Vladimir Pomjakushin[1], Philippe Borel[3], Cécile Tessier[3], Claire Villevieille[4*]

1. Laboratory for Neutron Scattering and Imaging, Paul Scherrer Institute, 5232 Villigen PSI, Switzerland

2. Electrochemistry Laboratory, Paul Scherrer Institute, 5232 Villigen PSI, Switzerland

3. SAFT, 111 Boulevard Alfred Daney, 33074 Bordeaux Cedex, France

4. Université Grenoble Alpes, Grenoble INP, LEPMI Laboratory, 38402 St Martin d'Hères, France

*Corresponding authors: denis.cheptiakov@psi.ch, claire.villevieille@gmail.com

Supplementary Note 1. The operando stroboscopic neutron diffraction mode

The idea to be able to look into the microscopic mechanisms of the phase transitions, and to characterize the structure of possible transient states of matter is not new, yet the obvious principal obstacle is the vanishingly short periods of time during which the hypothetical intermediate states of interest usually exist. Majority of the phase transformations in solid substances that would be a natural playground for neutron scattering studies, are occurring on the time scales of ps to ns. On the contrary, the phenomena occurring in mesoscopic systems are characterized by the time scales that are already in some cases closer to those we are living in. The spatially inhomogeneous (modulated on the mesoscopic scales) systems do display relaxation, diffusion and transition phenomena with characteristic time-scales sometimes on the order of seconds or even slower. This is where the (neutron) stroboscopic studies can find their application. For example, a good introduction to the principles and a nice set of application examples of the stroboscopic neutron diffraction studies is given in Ref [1].

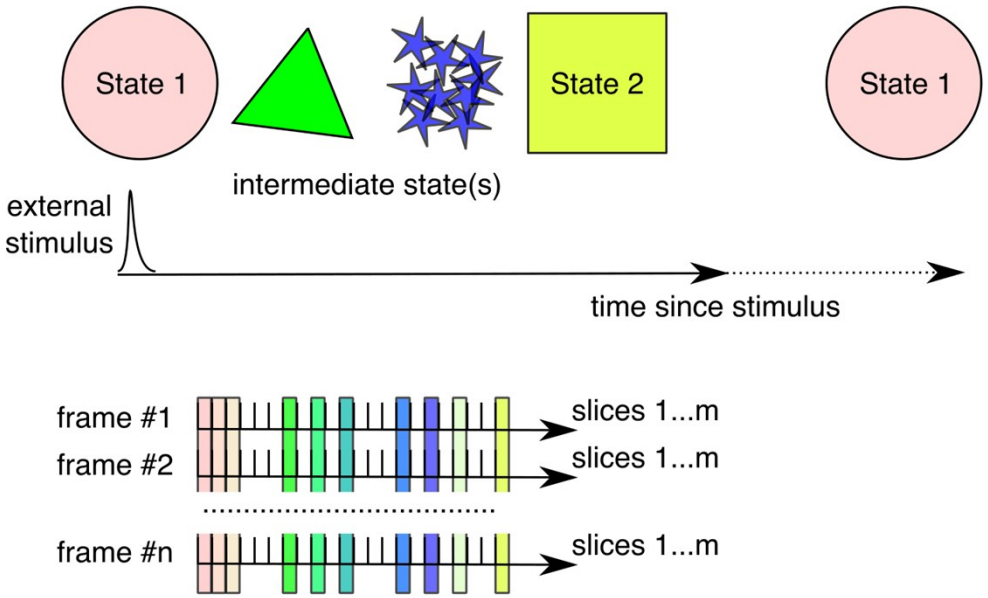

Figure S1. *Schematic representation of the stroboscopic neutron scattering experiment.*

Given the response of a system under study is repetitive, and excursions between the two states thereof are fully reproducible, it appears possible to utilize the stroboscopic techniques, and measure the scattering response as a function both of the natural scattering variable (e.g. the scattering angle), and of time since the perturbation that would cause the transition. A schematic representation of the principle is given in Figure S1. A system under study undergoes a transition caused by “external stimulus” from “state 1” (schematically represented as a circle) to the “state 2” (square), possibly also passing through some intermediate states (triangle, stars). Later on, the system either relaxes itself, or is being driven by some other external stimulus back to the “state 1”. For each of the scale units of the “time since stimulus” axis, the intensity would be very low, but having repeated the process a sufficient number of times, and binned together the corresponding patterns for each of these time slices since the external stimuli causing the transition, one would hope to collect sufficient counting statistics to make the qualitative, or even quantitative conclusions on the state of the system at these particular times. Hence, the hope is there to collect sound enough neutron diffraction data to ideally refine the parameters of the crystal structures of the compounds in the intermediate states. Clear, many conditions have to be fulfilled in order the

scheme to be functioning properly. The most important is that the process under study is really repetitive, otherwise the patterns corresponding to the times of “intermediate states” would no longer be really representative, in practice hindering obtaining any conclusive results. Further, there are some certain limitations on how the duration of external stimulus (of electric pulse front, or of the force application, or of the magnetic field ramp etc.) and the characteristic time of the system’s response would need to correspond to each other. Ideally, it is the duration of the stimulus that needs to be much shorter, such that the uncertainties in the “time since stimulus” variable would become insignificant. For the similar reason, complications may arise for the use of time-of-flight neutron diffraction in stroboscopic mode for rather short processes. Here, the time spans of the utilized neutron pulses should be much shorter that the time scale of the process under study.

Supplementary Figures

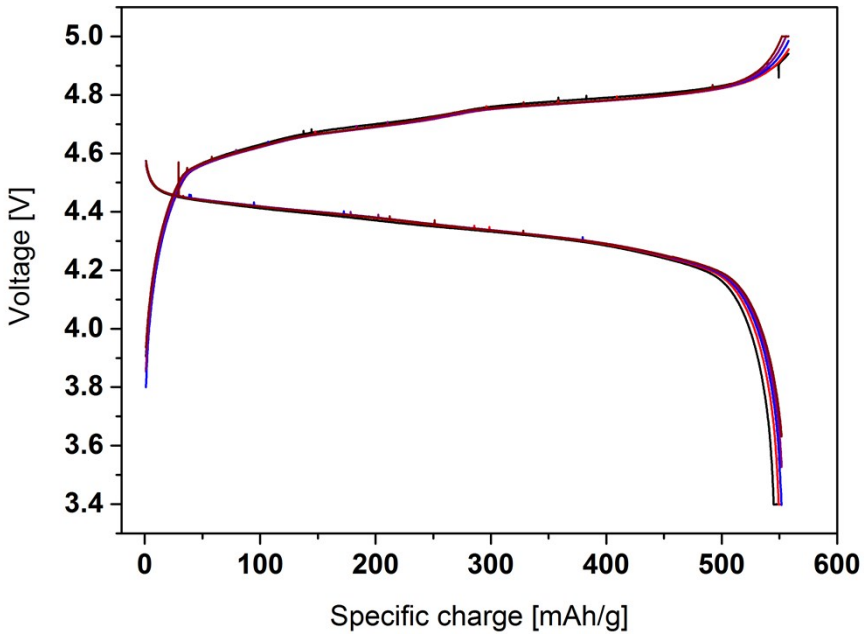

Figure S2. Comparison of the galvanostatic cycling curves of d-LNMO ($LiNi_{0.5}Mn_{1.5}O_4$) vs graphite (in custom-made cylindrical cell) measured at 1.1C rate at 25°C. The black curves represent the first galvanostatic curves and the dark red the 10^{th} cycle. The very nice overlap between the different cycles indicated that the cell is optimal for studying its components with the operando stroboscopic neutron diffraction mode.

Table S1. Refined crystal structure parameters of the d-LNMO phases (cathode material) at different states of charge of the cell. Results obtained from the refinements done on the stroboscopic data collected on the d-LNMO vs. graphite cell cycled at ~1.1C rate and binned over 1 minute time intervals. (4 charge cycles binned).

d-LNMO: assumed fixed composition: $LiNi_{0.5}Mn_{1.5}O_4$				
Space group: *Fd-3m (#227)*, Z=8, set of fixed reasonable parameters: Ni/Mn *16d (1/2,1/2,1/2), Biso=0.4 Å²*, occ(Ni:Mn)=1:3; Li *8a (1/8,1/8,1/8) Biso=1.5 Å²*, occ=1; O *32e (x,x,x), x=0.263 Biso=0.5 Å²*, occ=1				
Time since strobe start = time since beginning of charge (min)	1	40	57	
Remark	phase 1, fully discharged	phase 1, just before separating into phases 2 and 3	phase 2, half-filled Li site	phase 3, essentially Li-free
a (Å)	8.154 (1)	8.066 (4)	8.12931	8.004 (1)
Occ (Li)*	0.70 (13)	0.28 (17)	0.5	0.05 (17)

* due to a limited precision in determining the lithium content, any particular values for lithium occupation are averages over a few neighboring points; the complete results are shown in Figure 3 in the main text.

Tables S2. Crystal structure models used in the refinements based on the stroboscopic data collected on the d-LNMO vs. graphite cell cycled at ~1.1C rate and binned over 1 minute time intervals. (4 charge cycles binned). Parameters without supplied errors were fixed in the refinements.

C (Graphite), Strobo-slice #1 (the 1st minute after the start of charge, phase fraction of graphite in the anode material is 100%).

Graphite, Space Group $P6_3/mmc$, Z=4, a = 2.4607(1), c = 6.7200(3)			
Atom	Wyckoff site		
C1 C2	*2b* (0,0,1/4); and *2c* (1/3,2/3,1/4);	$B_{iso,}$ (Å^2) [1]	0.70 (4)

LiC_{18} (stage 3L), strobo-slice #15, anode material consists of LiC_{18} (84 (1)%wt.) and of graphite C (16 (1)%wt.). In order to reduce the number of refined parameters, all positional parameters were taken from our previous work[2], where the LiC_{18} phase has been studied in detail:

LiC_{18}, Space Group *P -6 2 m*, Z=1, a = 4.2709(2), c = 10.411(1)			
Atom	Wyckoff site		
Li	*1a (0,0,0)*	$B_{iso,}$ (Å^2)[2]	1.5
C1	*1b (0,0,1/2);*	$B_{iso,}$ (Å^2)[1]	0.76 (5)
C2	*3g (x,0,1/2);*	*x*	0.335
C3	*2d (1/3,2/3,1/2);*		
C4	*6i (x,0,z);*	*x*	0.341
		z	0.1777
C5	*6i (x,0,z);*	*x*	0.659
		z	0.1777

[1] For each particular strobo-slice (for every particular time since the beginning of charge), the B_{iso} values for all carbon atoms in all graphite derivative phases were refined with constraint to equality. The reason is to keep as little number of refined parameters as possible, and only follow the values of the principal, decisively changing parameters.

[2] B_{iso} value for Li atom was fixed at a reasonable value of 1.5 Å^2. The weakness of Li scattering does not allow for a safe refinement of B_{iso} in presence of so many phases.

LiC_{12} (stage 2), strobo-slice #39, weight-referenced composition of anode material: graphite C: 12 (1)%, LiC_{18}: 13 (2)%, LiC_{12}: 69 (2)%, LiC_6: 6 (1)%.

LiC_{12}, Space Group *P6/mmm*, Z=1, a = 4.2861(2), c = 7.0437(7)			
Atom	Wyckoff site		
C	*12n (x,0,z);*	*x*	0.337
		z	0.2333 (5)
		$B_{iso,}$ $(Å^2)^1$	1.00(6)
Li	*1a (0,0,0)*	$B_{iso,}$ $(Å^2)^2$	0.84 (4)

LiC_6 (stage 1), strobo-slice #57 weight-referenced composition of anode material: graphite C: 13 (1)%, LiC_{12}: 50 (2)%, LiC_6: 37 (1)%. In order to reduce the number of refined parameters, the x-coordinate of C atom was fixed to the value from our previous work[2], where the LiC_6 phase has been studied in detail:

LiC_6, Space Group *P6/mmm*, Z=1, a = 4.3133(2), c = 3.6982(5)			
Atom	Wyckoff site		
C	*6k (x,0,1/2);*	*x*	0.3307
		$B_{iso,}$ $(Å^2)^1$	0.99 (5)
Li	*1a (0,0,0)*	$B_{iso,}$ $(Å^2)^2$	1.5

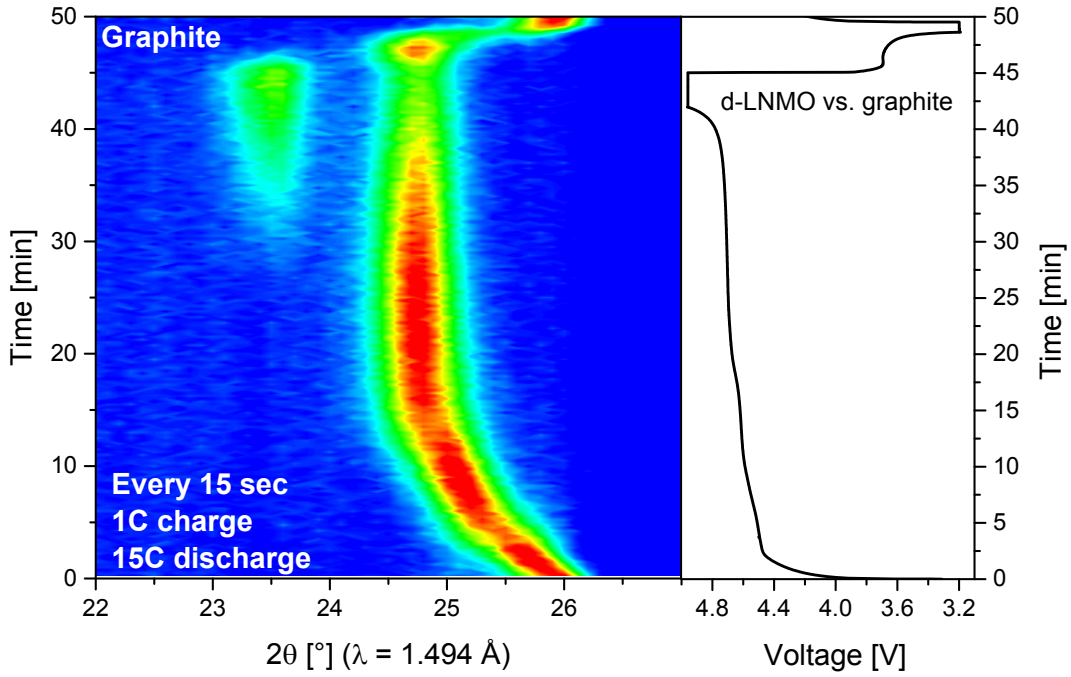

Figure S3. Contour plot representation of the operando stroboscopic neutron diffraction measurement of a d-LNMO vs graphite cell, 1.33C/15C rates for charge/discharge, respectively: (left) the (002) graphite reflection (pattern every 15 sec), (right) the galvanostatic cycle of d-LNMO vs graphite.

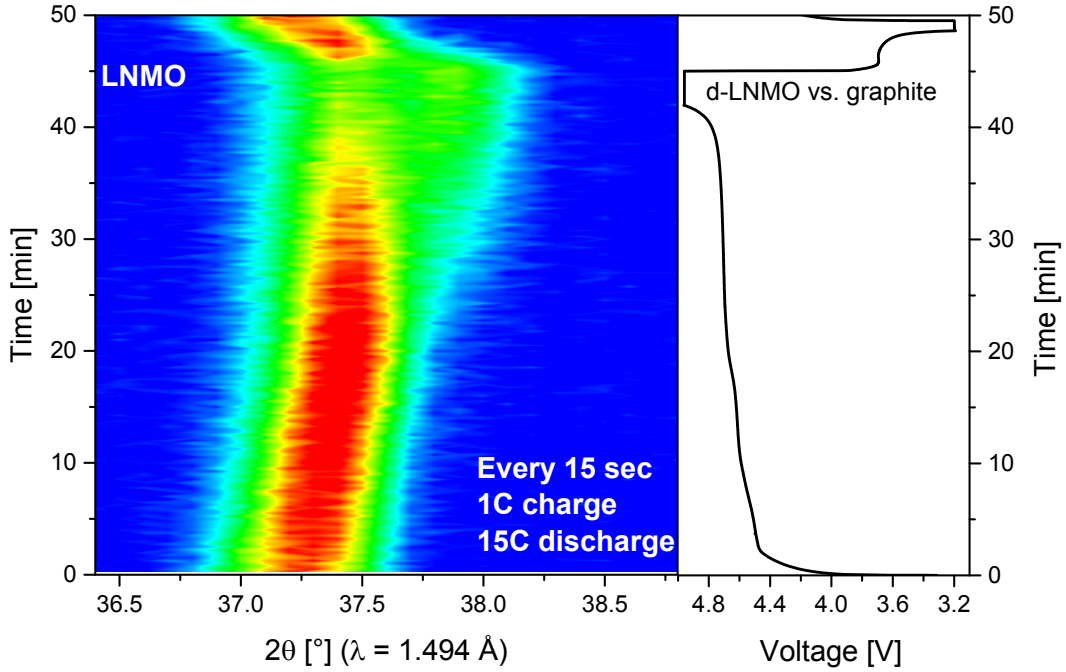

Figure S4. *Contour plot representation of the operando stroboscopic neutron diffraction measurement of a d-LNMO vs graphite cell, 1.33C/15C rates for charge/discharge, respectively: (left) the (222) LNMO reflection (pattern every 15 sec), (right) the galvanostatic cycle of d-LNMO vs graphite.*

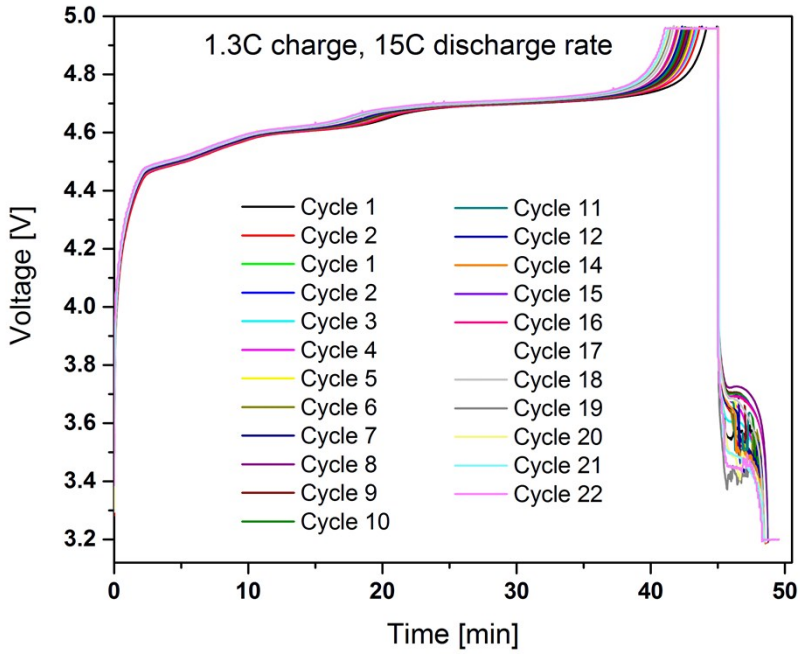

Figure S5. *Galvanostatic curves of a d-LNMO vs graphite cell at 1.33C/15C rate for charge/discharge respectively (the voltage fluctuations during discharge is due to inaccuracy of the potentiostat device).*

[1] G. Eckold, H. Gibhardt, D. Caspary, P. Elter, K. Elisbihani, Z. Kristallogr. 218, 2003, 144, DOI: 10.1524/zkri.218.2.144.20670

[2] L. Boulet-Roblin, P. Borel, D. Sheptyakov, C. Tessier, P. Novák, C. Villevieille, J. Phys. Chem. C 2016, 120, 17268, DOI: 10.1021/acs.jpcc.6b05777